Research, Society and Development, v. 13, n. 1, e4113144735, 2024
(CC BY 4.0) | ISSN 2525-3409 | DOI: http://dx.doi.org/10.33448/rsd-v13i1.44735

Evaluation of the mandibular canal in stereolithographic biomedical prototypes

Avaliação do posicionamento do canal mandibular em protótipos biomédicos esterelitográficos

Evaluación del posicionamiento del canal mandibular en prototipos biomédicos estereolitográficos

Received: 12/27/2023 | Revised: 01/05/2024 | Accepted: 01/06/2024 | Published: 01/08/2024

Andressa Ferreira Martins
ORCID: https://orcid.org/0009-0002-6002-8497
Universidade Paulista, Brazil
E-mail: andressaf.martins@hotmail.com
Igor Ednardo Santos Cézar
ORCID: https://orcid.org/0009-0006-2435-5780
Escola Baiana de Medicina e Saúde Pública, Brazil
E-mail: drigorcezar@hotmail.com
Lívia Prates Soares
ORCID: https://orcid.org/0000-0003-4931-1195
Escola Baiana de Medicina e Saúde Pública, Brazil
E-mail: liviapsoares@hotmail.com
Maylon Luciano Garcia Barbosa
ORCID: https://orcid.org/0009-0006-0187-8191
São Leopoldo Mandic, Brazil
E-mail: maylonlgarcia@gmail.com

Abstract
Objective: The purpose of this research was to evaluate through an experimental study the positioning accuracy of the mandibular canal of sterolithographic prototypes, also comparing them with the dry human jaws which served as the basis for their manufacture. Material and methods: 10 human jaws (20 mandibular canals) were submitted to computed tomography examination and reproduced in transparent stereolithographic biomodels with evidence of the mandibular canals, so that linear measurements between previously determined could be performed and compared. For data analysis was used the t test of paired samples, and p values < 0.05 were considered statistically significant. Results: The results obtained revealed that there is a statistically significant difference of approximately 10.21% between the measurements obtained in dry mandibles and biomodels. Finally, the similarity and variability of intra and inter-examiner probabilities were evaluated, and a strong agreement was found in both cases, demonstrating the reproducibility of the method used. Conclusion: More studies are needed before using the mandibular canal of stereolithographic prototypes as a parameter for clinical use.
Keywords: Anatomy; Sterelithography; Mandible; Mandibular nerve; Tomography.

Resumo
Objetivo: A proposta desta pesquisa foi avaliar, através de um estudo experimental, a precisão do posicionamento do canal mandibular de protótipos estereolitográficos, comparando-os com as mandíbulas humanas secas que serviram de base para sua confecção. Material e métodos: 10 mandíbulas humanas (20 canais mandibulares) foram submetidas ao exame de tomografia computadorizada e reproduzidas em biomodelos estereolitográficos transparentes com evidenciação dos canais mandibulares para que medições lineares entre pontos pré-determinados pudessem ser realizadas e comparadas. Para análise dos dados foi utilizado o teste t de amostras pareadas, e valores de p < 0.05 foram considerados estatisticamente significativos. Resultados: Os resultados obtidos demonstraram que há uma diferença relativa estatísticamente significante de aproximadamente 10,21% entre as medidas obtidas em mandíbulas secas e biomodelos. Por fim, foi avaliada a similaridade e variabilidade das medições intra e inter-examinadores, e constatou-se uma forte concordância em ambos os casos, demonstrando a reprodutibilidade do método utilizado. Conclusão: Mais estudos são necessários antes que se utilize o canal mandibular de protótipos estereolitográficos como parâmetro para finalidade de uso clínico.
Palavras-chave: Anatomia; Estereolitografia; Mandibula; Nervo mandibular; Tomografia.

Resumen
Objetivo: El objetivo de este estudio fue evaluar la precisión del posicionamiento de los conductos mandibulares en prototipos estereolitográficos comparándolos con las mandíbulas humanas secas sobre las que se realizaron. Material y métodos: 10 mandíbulas humanas (20 conductos mandibulares) fueron sometidas a una tomografía computerizada y reproducidas en biomodelos estereolitográficos transparentes con los conductos mandibulares visibles para poder tomar medidas lineales entre puntos predeterminados y compararlas. Para analizar los datos se utilizó la prueba t de

muestras pareadas, y los valores p < 0,05 se consideraron estadísticamente significativos. Resultados: Los resultados obtenidos mostraron que existe una diferencia relativa estadísticamente significativa de aproximadamente el 10,21% entre las medidas obtenidas en mandíbulas secas y biomodelos. Por último, se evaluó la similitud y la variabilidad de las mediciones intra e interexaminadores y se observó una gran concordancia en ambos casos, lo que demuestra la reproducibilidad del método utilizado. Conclusión: Son necesarios más estudios antes de que el canal mandibular de los prototipos estereolitográficos pueda utilizarse como parámetro para uso clínico.
Palabras clave: Anatomía; Estereolitografía; Mandíbula; Nervio mandibular; Tomografía.

1. Introduction

The science has sought to provide support to the continuous challenge of dentists in offering excellence in the precision of diagnosis, planning and treatment of craniofacial diseases. Not by chance, there is a large number of researches and advances in biomedical technology, especially in the field of imaging exams for the planning of advanced therapies (Escóssia et al., 2008; Rouzé et al., 2022). From complex reconstructive surgeries to delicate surgeries with dental implants, they have benefited of this progress and offered answers through their needs and results so that a continuous advance in this field happens.

The importance and complexity of the craniofacial region have required more than conventional two-dimensional radiographic examinations to obtain useful images for an accurate diagnosis. These exams alone do not provide a definition or three-dimensional overview of the anatomical region of interest, impairing the possibilities of reaching a correct understanding about a disease (Escóssia et al., 2008; Nigro & Francischone, 2010).

The advent of computed tomography (CT) reduced part of the imperfection of the exams available until then and allowed the emergence of new paths for the health area, expanding the quality, definition and angles from which an anatomical structure could be analyzed (Alamri et al. 2012; Rajakeerthi & Nivedhitha, 2019; Alageb et al., 2020; Souza et al, 2021; Zandi et al., 2021; Viegas et al., 2021). This is still not an unlimited or universal diagnostic resource, and for some more complex cases, printed two-dimensional CT images can also be difficult to assess (Escóssia et al., 2008).

Currently, there are biomedical prototypes, enabling a visualization three-dimensional, life-size as if you were holding the anatomical piece to be operated on in your hands. This makes it possible to eliminate doubts regarding the diagnosis, allowing the evaluation of curvatures and sudden variations in height and volume, complete notion of proportions, inclinations, relative evaluation between the parts and a unique tactile perception (Freitas et al., 2010).

They have been widely used in dentistry, especially as an aid in diagnosis, study for surgical planning, simulation of procedures, anatomo-topographic analyses, manufacture of dental and facial prostheses, as a teaching resource, communication material between the team and with the patient, parameter for later comparisons, preparation of bone grafts, orthognathic surgeries and osteogenic distraction (Freitas et al., 2010). Rapid prototyping is also used to print surgical guides with the aim of improving precision in the installation of dental implants (Akhila et al. 2019; Di Giocomo et al., 2005).

Different materials are used to make prototypes and they vary according to the purpose of production and the prototyping technique to be used. Based on the 3D virtual model created from the image scan, rapid prototyping systems build biomodels using two main methods: by subtracting material, using a variety of types of cutters, reducing it to the physical replica of the model; or by sequential construction, through the successive addition of thin layers of specific materials, such as plastics, resins, ceramics, metals, among others, until an analog copy of its original is formed (Volpato et al., 2007; Jandyal et al., 2022; Lahoti et al., 2020).

Among the types of biomodels available on the market, there are those made using the stereolithography method, which is based on the polymerization of a photosensitive resin in layers using an ultraviolet laser beam. These parts have the advantages of being quick to make, transparent and allowing internal anatomical structures of interest to be highlighted (Chilvarquer et al. 2004). In order for prototypes to be suitable for the vast majority of their applications, it is an important prerequisite that there be exacting dimensional accuracy in the reproduction of the anatomical part that gave rise to them. Biomodels made using the stereolithography method have been described as one of the most reliable alternatives in terms of dimensional fidelity in the reproduction of an anatomical part and target structures (Queiroz, 2022). However, there is a lack of studies in the scientific literature evaluating the degree of accuracy of the internal structures shown in this type of biomodels. For this reason, the aim of this study was to compare the positioning of the mandibular canal in a dry mandible with that of its stereolithographic prototype.

2. Methodology

This study protocol was approved by the research ethics committee on the Brazil platform (CAAE: 13556513.1.0000.5544). The dried human mandibles studied were provided by the Morphology Department of the Metropolitan Union of Education and Culture (UNIME).

Ten human dry mandibles were selected considering as inclusion criteria the presence of bilateral posterior edentulism or total edentulism, healed posterior alveolar bone (from the first premolar onwards), the presence of integrity of the anatomical structure of the body, absence of fractures and surface bone defects. Each mandible was randomly identified with a number from 01 to 10. The jaws were centered with their bases parallel to the plane of the support, using a laser light beam as a reference for this purpose (Figure 1).

Figure 1 - Laser beams guiding the centralized positioning of the mandible on the horizontal support in the scanner.

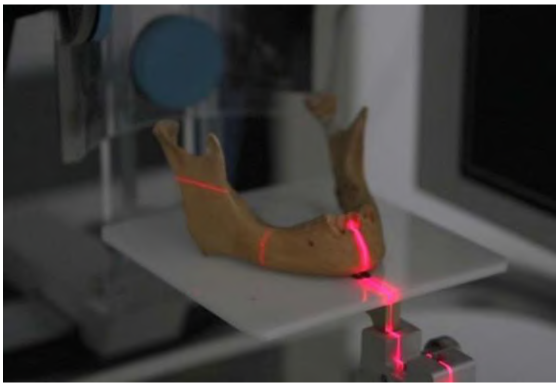

Source: Authors (2023)

As can be seen in Figure 1, a scout view was carried out in order to visualize whether the positioning of the jaw on the support was support was adequate.

Once identified, all the mandibles were subjected by the same operator to a computerized tomography scan, carried out on the i-CAT® cone beam computerized tomography scanner for dental applications (Imaging Sciences International, Philadelphia, USA). The scan was carefully carried out on a standard fixed surface, with its bases parallel to the bracket plane, using a laser light beam for this purpose as a reference.

Following the specifications recommended in the literature (Nigro et al., 2010), the CT scanner was configured for maximum image acquisition resolution, in order to obtain clear images in which the external boundaries and internal structures could be easily located, offering greater use for making the prototypes.

The FOV used was 6 cm, with reconstruction intervals of 0.2mm for each axial section and voxel size. The energy factors used were 120 kVp and 36 mAs. The files were stored in DICOM format and sent online to BioParts (BioParts - Prototipagem Biomédica, Brasília - DF, Brazil) to make stereolithographic prototypes with evidence of the mandibular canals.

The prototypes were then made as three-dimensional solid resin models using the SLA-250 device (3DSystems, Valencia, CA, USA). The mandibular canal was inserted with a different coloring as a second 3D object superimposed on the first (Figure 2).

Figure 2 - Mandible and its stereolithographic prototype with the mandibular canal in evidence.

Source: Authors (2023).

In order to this structure to be highlighted with a different color, a longer laser scan was carried out in the area. This allowed us to observe this structure through the transparency of the prototype's main structure.

Using two self-curing colorless acrylic resin matrices, each mandible was cut out in four places between the mental foramen and the internal angle of the ramus, with two sections per hemiarch. The resin matrices were then removed from the mandible segments and fitted to the equivalent biomodels (Figures 3 and 4).

Figure 3 - Upper and lower matrices, made from acrylic resin, with a sheet of wax 07 interposed to isolate their edges.

Source: Authors (2023).

Figure 4 - Upper and lower matrices properly fitted to the into the model after being finished.

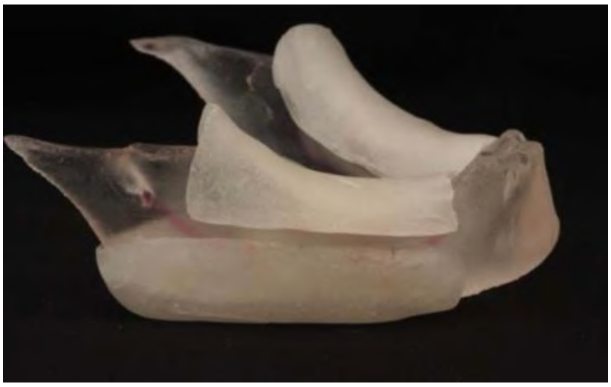

Source: Authors (2023).

The use of these resin matrices allowed the spacing between the fragments to clearly identify where the section was to be reproduced on the model in figures 3 and 4.

With the matrices in place, each mandible was cut out in four places, between the mental foramen and the internal angle of the ramus, with two sections per hemiarch (Figures 5 and 6).

Figure 5 - Cutting being started with the aid of micro saws.

Source: Authors (2023).

Figure 6 - First section made, subdividing the jaw and guide dies.

Source: Authors (2023).

The cutouts were made using a Ney-type hacksaw and micro-saws (Bordente - São Paulo - Brazil), starting at the upper end, perpendicular to the body and towards the mandibular base, tangent to the entire structure.

The resin matrices were then removed from the mandible segments and fitted into the into the equivalent biomodels. The spacing between the cut-out matrix fragments the section point to be reproduced on the biomodels (Figure 7).

Figure 7 - Matrix segments embedded in the model, making it clear where the cut-out point is to be replicated.

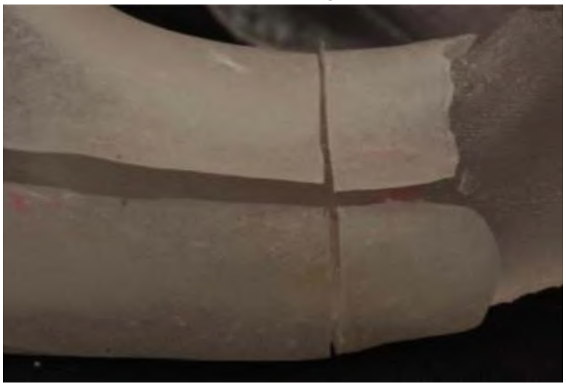

Source: Authors (2023).

Figure 7 shows the reproducibility of the cuts, which could be made similarly in the mandibles and in their respective biomodels.

Ivory matrix holder n. 8 (JON - Produtos Odontológicos - São Paulo - SP), and stainless steel 5mm stainless steel matrix tape (JON - Produtos Odontológicos - São Paulo - SP) were used to stabilize the resin matrix fragments and reinforce the cut-out boundaries, preventing microsaw deviations and maintaining the equivalence of the cutting region between the mandible and its prototype (Figures 8).

Figure 8 - Matrix tape stabilizing the guides and preventing deviations of the micro saw at the cutting interface interface.

Source: Authors (2023).

The ivory die holder prevented the microsaw from deviating and maintained the equivalence of the cutting region between the jaw and its prototype.

At the end of the four cut-outs, each mandible and model was subdivided into 5 parts, with 4 axial surfaces for evaluation (Figure 9). Each mandible fragment was promptly labeled with self-adhesive stickers identifying them.

Figure 9 - Mandible and its respective biomodel sectioned into 4 regions, and their fragments identified.

Source: Authors (2023)

Markings were made with graphite pencils with 0.5mm tips, first on the anatomical part, then transferred to the matrix, and then transported to the matrix, and then transported to the bio-model (Figures 10 and 11).

Figure 10 - Markings identifying the measurement points, transferred from the anatomical specimen to the matrix fragments.

Source: Authors (2023)

Figure 11 - Matrix repositioned on the fragment of the fragment, allowing the markings to be transmitted at the same points as on the dry mandible.

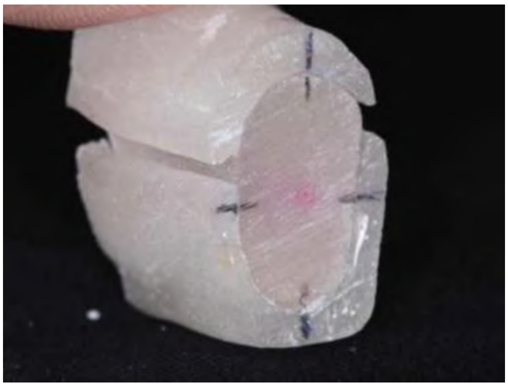

Source: Authors (2023)

The acrylic matrices, in addition to serving as cutting guides, were used to transfer the markings to standardize the measurement reference points from the mandible to the model.

The measurements corresponded to the shortest distance in height and width between the points marked on the external boundaries of the part (mandible or biomodels) and the mandibular canal (Figure 12).

Figure 12 - Measurement of SV using a digital caliper on a dry mandible

Source: Authors (2023).

As shown in figure 12, four measurements were taken for each cutting surface, as follows: VS (Upper Vertical: Distance in height between the mandibular canal and the superior wall); VI (Lower Vertical: Distance in height between the mandibular canal and the inferior wall); HL (Horizontal Lingual: Distance in width between the mandibular canal and the lingual wall); HV (Horizontal Vestibular: Distance in width between the mandibular canal and the buccal wall).

Data was analyzed using Lin's Coefficient to assess the reproducibility of intra- and inter-examiner measurements, with 95% confidence intervals. For each linear measurement, the mean absolute and relative dimensional errors were calculated using the formulas: Mean Absolute Difference = Jaw measurement - Biological model measurement and Relative Difference = Jaw Measurement – Biological model Measurement X 100 / Jaw Measurement. These formulas were found in studies by Choi et al., 2002; Ibrahim et al., 2009 & Bomfim, 2017.

Considering the averages of the linear measurements obtained, the Student's t-test was applied to compare sets of measurements at a 5% significance level.

In total, 4 measurements were taken for each cutout face, which amounted to 16 measurements per jaw. As a total of 10 mandibles and their 10 biomodels were measured, a total of 320 measurements were obtained by each examiner in each of their evaluations. All measurements were recorded twice by two observers, with an interval of 7 to 10 days between them, resulting in a total of 1280 measurements.

3. Results

Lin's coefficient was used to assess the consistency and reproducibility of the measurements. For the analysis of intra-examiner variability, the test showed very strong agreement for both assessor 1 (0.9992 for mandible measurements and 0.9989 for prototype measurements) and assessor 2 (0.9991 for mandible measurements and 0.9984 for prototype measurements).

Inter-rater variability was then assessed. Lin's test showed that between assessors 1 and 2 the correlation coefficient was 0.9977 for mandible measurements and 0.9979 for prototype measurements, demonstrating high agreement and indicating the reproducibility of the method used (Table 1).

(CC BY 4.0) | ISSN 2525-3409 | DOI: http://dx.doi.org/10.33448/rsd-v13i1.44735

Table 1 - Results of applying Lin's coefficient to all measurements. Data subdivided into mandibles and prototypes, comparing intra- and inter-examiner measurements.

	Intra-evaluator		Inter-evaluator
	Avaluator 1	**Avaluator 2**	**Avaluator 1 e 2**
Jaws	0,9992	0,9989	0,9977
Prototypes	0,9991	0,9984	0,9979

Source: Authors (2023).

For each linear measurement, the average absolute dimensional error was calculated as the difference between the average of the values obtained from the measurements taken on the dry jaws and the average value found on the prototypes, expressed in millimeters. Next, the relative differences between the anatomical specimen and the prototype were also calculated, using the mandible as a standard reference and with the result expressed as a percentage (tables 2 and 3). A paired samples t-test was used and p-values of less than 0.05 were considered statistically significant.

Table 2 - Absolute and relative means of the differences found between the linear measurements of the mandible and prototype subdivided by hemi-arch. Statistical difference with probability of error of 0.05 for significance level.

Jaw/Prototype	Hemi-arch	Average absolute difference (mm)	Average relative difference (%)	Significance
1	**Right**	0,74	12,83	p<0,05
	Left	0,67	11,53	p<0,05
2	**Right**	0,62	13,07	p<0,05
	Left	0,47	10,17	p<0,05
3	**Right**	0,71	22,60	p<0,05
	Left	0,42	13,45	p<0,05
4	**Right**	0,08	11,06	p<0,05
	Left	0,19	14,82	p<0,05
5	**Right**	0,39	07,37	p<0,05
	Left	0,53	13,08	p<0,05
6	**Right**	0,09	00,75	p<0,05
	Left	0,49	11,81	p<0,05
7	**Right**	0,42	11,16	p<0,05
	Left	0,24	08,94	p<0,05
8	**Right**	0,29	04,01	p<0,05
	Left	0,48	09,17	p<0,05
9	**Right**	0,47	07,45	p<0,05
	Left	0,49	08,16	p<0,05
10	**Right**	0,06	07,07	p<0,05
	Left	0,26	05,76	p<0,05
Overall average		**0,41**	**10,21**	**p<0,05**

Source: Authors (2023).

Evaluating the difference between the means of the measurements obtained in each hemi-arch of the mandible and prototype, it can be seen that only in the measurements taken in 3 of the 20 hemi-prototypes was there no statistically significant difference in relation to the measurements obtained in the dry hemi-mandibles (Table 2).

Table 3 - Absolute and relative means of the differences found between the linear measurements of each mandible and prototype. Statistical difference with probability of error of 0.05 for significance level.

	Mean Absolute Dimesional Error (mm)	Mean Relative Dimensional Error (%)	Significance
Prototype 1	0,71	12,18	p<0,05
Prototype 2	0,55	11,62	p<0,05
Prototype 3	0,57	18,02	p<0,05
Prototype 4	0,14	12,94	p<0,05
Prototype 5	0,46	10,22	p<0,05
Prototype 6	0,29	6,28	p<0,05
Prototype 7	0,33	10,05	p<0,05
Prototype 8	0,39	6,59	p<0,05
Prototype 9	0,48	7,81	p<0,05
Prototype 10	0,16	6,41	p<0,05
OVERALL AVERAGE	0,41	10,21	p<0,05

Source: Authors (2023).

When each prototype-jaw relationship was analyzed, significant differences were found in all samples, with a mean absolute error and a mean relative error of 0.41mm and 10.21%. The results expressed as positive values show that the measurements on the prototype are generally greater than on the mandible, so there is a tendency to overestimate the distance between the edges of the part and the mandibular canal on the biomodels (Table 3).

The differences in the distances measured in the most anterior sections of the prototypes were compared separately from those measured in the most posterior region of the prototypes, in relation to their corresponding measurements obtained in the dry mandibles. A similar analysis was carried out by subdividing the horizontal measurements and the vertical measurements. The data is shown in tables 4 and 5.

Table 4 - Average absolute and relative differences by cutting region.

	Average absolute Difference (mm)	Average Relative Difference (%)
Anterior	0,42	10,11
Posterior	0,39	10,31

Source: Authors (2023).

Table 5 - Average absolute and relative differences by measurement axis.

	Average Absolute Difference (mm)	Average Relative Difference (%)
Horizontal	0,38	13,79
Vertical	0,44	6,63

Source: Authors (2023).

In addition, the measurements were segmented by type of measurement taken. The dimensional error was assessed by comparing all the linear measurements taken in the different directions. In addition, standard deviations were calculated for all the mean measured values (Table 6).

Table 6 - Mean absolute and relative differences, standard deviation and maximum and minimum error found for each type of measurement taken.

	Mean Absolute Error (mm)	Mean Relative Error (%)	Minimum Absolute Error (mm)	Maximum Absolute Error (mm)	Standard Deviation
VS	0,33	4,67	0,03	2,16	0,658
VI	0,54	8,59	0,03	2,44	0,689
HV	0,34	7,85	0,00	1,69	0,415
HL	0,41	19,73	0,00	1,89	0,473

Source: Authors (2023).

4. Discussion

Locating the mandibular canal accurately is a critical prerequisite for many surgical procedures performed on the mandible. The position of this canal should be identified as a safety and preventative measure in previous assessments in surgeries to remove impacted third molars, install implants, lateralize the inferior alveolar nerve, in block graft surgeries when this is a recipient or donor area, among other procedures (Kumar et al., 2020).

In implant surgery, for example, every millimeter is crucial in the diagnosis to avoid damaging the inferior alveolar nerve. This is a serious concern, as an inadvertent surgical incursion through the mandibular canal leads to a high chance of hemorrhage, potential formation of fibrous tissue with a consequent smaller osseointegration area around the implant, as well as uncomfortable changes in the sensory function of the nerve such as hyperesthesia, paresthesia or chronic anesthesia, which can affect the patient's quietness and quality of life (Queiroz, 2012).

A variety of tests and diagnostic techniques have been used to detect and estimate the positioning of the mandibular canal, however, studies have shown the lack of precision and reliability of radiographs for this purpose (Nigro et al., 2010). On the other hand, the advent of three-dimensional imaging tests has made determining the location of the mandibular canal much more reliable (Alamri et al., 2012) while stereolithography appears to be another possibility for determining the positioning of this canal, by showing this structure on a palpable physical model (Freitas et al., 2010; Santana, 2012).

If many articles cite the high degree of fidelity of stereolithographic biomodels (Escossia, 2008; Chilvarquer, 2004; Choi, 2002; Voet et al., 2018) and if their applications include the possibility of their being used to guide and simulate surgical procedures, eliminate diagnostic doubts and plan advanced surgeries (Freitas 2010; Chilvarquer, 2004; Singare et al., 2009), it would not be absurd to deduce that the internal structures shown in these prototypes could also be used for these purposes. However, the degree of accuracy of the positioning of these internal structures has not yet been quantified. Therefore, discovering the level of fidelity of this resource will help define whether this artifact can be used for purposes that require greater precision, or whether its indication is restricted to mere didactic and communication applications.

In the scientific literature, some studies have evaluated the fidelity of biomedical prototypes (Choi et al., 2002; Ibrahim et al., 2008; Santana et al., 2012; Asaumi et al., 2001; Safira et al., 2011; Tarf et al., 2011; Shahbazian et al., 2010), but the difference in this study was that it proposed to measure the fidelity of the positioning of an internal structure evidenced in biomedical prototypes, while practically all the studies cited sought to evaluate the inaccuracy of biomodels based on comparisons of measurements made at superficial points. Santana et al, in 2012, Tarf et al. (2011), Safira et al. (2011), carried out comparative measurements of prototypes in relation to their respective anatomical structures and also obtained significant mean differences. Other studies, such as those by Ibrahim et al. (2009), Shahbazian et al. (2010) and Murugesan et al. (2011), also sought to assess the degree of fidelity of prototypes of various types, comparing distances between points on their surfaces to the equivalents on the anatomical structures that gave rise to them or on their virtual 3D models, and came up with results with average percentage errors ranging from 0.13% to 4.03%. The vast majority of studies aimed at estimating how accurate biomodels are compare measurements taken at pre-defined anatomical points on their surface only. Furthermore, unlike many of these studies (Kumar et al., 2020; Gupta et al., 2021; Safira et al., 2011) we used dry human mandibles to simulate the in vivo situation, and the measurements taken on these were considered a control for all comparisons.

Unlike the aforementioned studies, Di Giacomo et al (2005), followed a different methodology and evaluated the clinical application of the stereolithographic surgical guide model for implant installation. Comparing post-installation CT scans of implants that had been planned and executed with the printed guides, it was observed that there was an approximate discrepancy of 7.25 +/- 2.67 degrees in the inclination of the implants, the difference in the position of the upper part of the implant positioned was 1.45 +/- 1, 42mm and of 2.99 +/- 1.77mm at the apex of the installed implant when compared to the planning that had been carried out before its installation, indicating that there was a difference in the positions found compared to the digital planning previously carried out, aided in execution by the steriolithographic guide.

Other studies need to measure the dimensional error of internal structures, such as the mandibular canal, so that a direct comparison of results can be made. In general, the dimensions measured in the biomodels were significantly greater than those of the dry mandibles in our study.

The methodology used in this study showed strong intra- and inter-examiner agreement, as demonstrated by the statistical analysis of more than 1,200 measurements. This result shows that the difficulties involved in locating landmarks and possible human error in the measurements had little influence on the results of our work. A plausible explanation for the significant difference found between the measurements of the prototype and the mandible may lie in the incomplete reproduction of the shape of the mandibular canal in the biomodels. Through their cross-sections, we observed that while the canals of dry mandibles were shaped differently, they were invariably circular in the biomodels. The prototypes seem to adequately reproduce the path of the mandibular canals, but do not seem to be able to be faithful to their volume and shape, with these characteristics being standardized regardless of how they appear in the anatomical pieces from which they originated.

Of course, this standardization prevents the outer limits of the mandibular canal from being adequately respected and reproduced, because if the cross-section of the canal is a circle for any prototype, this could potentially make it differ from what is the actual shape found in the mandibles. This also partly explains the variation in relative error found between different jaws and prototypes, especially in the more extreme results of our study. We observed, for example, that in the right hemi-arch of mandible 03, an average relative error of 22.60% occurs with its prototype, while the comparison between the right hemi-arch of mandible 06 and its prototype showed an average relative error of 0.75%.

While agreeing on the premise that precision is essential for the applicability of biomodels, few authors have dared to quantify, and differ when estimating, an acceptable margin of error for prototypes. Asaumi et al. (2001), calculated that a relative variation of 2% is acceptable and not enough to make it unfeasible to use in assisting surgical procedures, while Kragskov et al. (1996) and Silva et al. (2008) considered the precision of 3.59% and 2.67% found in their studies to be optimal for the same purpose.

In implantology, for example, the VS measurement is of greater interest because it is the measurement of the bed available for the implant. Although the mean absolute error for this measurement is only 0.33mm, the dispersion of the values found in relation to the mean cannot be disregarded.

In this specialty, its applicability must be carefully assessed, as any millimeter is crucial and has an impact that can alter important therapeutic decisions. If biomodels are to be used merely as a teaching resource and to communicate with the patient, a greater magnitude of discrepancy can still be considered negligible (Freitas et al., 2010).

Further studies to advance this field and compare with our findings are highly recommended. A study of a similar nature and purpose would allow for a direct comparison of results with other companies responsible for manufacturing the biomodels, and/or the software and operator used to dermark the mandibular canal in the virtual model, resulting in new discrepancy values, generating subsidies for a comparison with the present study.

5. Conclusion

It is concluded that, based on the methodology used, this study provides a new view of internal structures replicated by biomodels. The strong agreement between the evaluators in all the measurements taken showed the applicability of the chosen methodology, highlighting the need for further studies to reveal the reliability of stereolithographic models as a parameter for clinical use. The divergence found in this study suggests caution in the application of this technology and alerts us to the need for further studies in this area.

In view of the divergence found between the anatomical parts and the parts generated by stereolithography, we suggest studies that evaluate alternative methods of measurement, seeking to assess whether the same distortion found in the internal structures of the model would also be found in the total structure reproduced by the additive stereolithographic method.

References

Akhila, A., Nandakishore, B., Miriam, M., Anil, S., Abhinav, M., & Fares, A. (2019). Rapid prototyping: An innovative technique in prosthodontics. *International Journal of Preventive and Clinical Dental Research*, 6(2), 46. https://doi.org/10.4103/inpc.inpc_16_19

Asaumi, J., Kawai, N., Honda, Y., Shigehara, H., Wakasa, T., & Kishi, K. (2001). Comparison of three-dimensional computed tomography with rapid prototype models in the management of coronoid hyperplasia. *Dento Maxillo Facial Radiology*, 30(6), 330–335. https://doi.org/10.1038/sj/dmfr/4600646

Bioparts – Prototipagem Biomédica. (n.d.). https://bioparts.com.br/?gclid=EAIaIQobChMIga3Gq_KcgwMVqFhIAB2wTQS7EAAYASAAEgIO5vD_BwE

Bomfim, R. T. (2017). Avaliação da acurácia de reconstruções panorâmicas geradas a partir de tomografia computadorizada: estudo experimental in vitro com mandíbulas secas humanas. Repositoriohml.ufba.br. https://repositoriohml.ufba.br/handle/ri/23513

Chilvarquer, I., Chilvarquer, L. W., Hayek, J. E., & Pinto, A. V. de S. (2004). A estereolitografia na Implantodontia avançada: conceitos, indicações e usos. *ImplantNews*, 69–72. https://pesquisa.bvsalud.org/portal/resource/pt/lil-405747

Choi, J.-Y., Choi, J.-H., Kim, N.-K., Kim, Y., Lee, J.-K., Kim, M.-K., Lee, J.-H., & Kim, M.-J. (2002). Analysis of errors in medical rapid prototyping models. *International Journal of Oral and Maxillofacial Surgery*, 31(1), 23–32. https://doi.org/10.1054/ijom.2000.0135

Freitas, S. A. P., Costa, P. M., & Ribeiro, R. C. (2010). The Use of biomedic prototyping in dentistry Uso da prototipagem biomédica em Odontologia. *Odontol. Clín.-Cient*, 9(3), 223–227. http://revodonto.bvsalud.org/pdf/occ/v9n3/a08v9n3.pdf

Giacomo, G. A. P. D., Cury, P. R., Araujo, N. S. de, Sendyk, W. R., & Sendyk, C. L. (2005). Clinical Application of Stereolithographic Surgical Guides for Implant Placement: Preliminary Results. *Journal of Periodontology*, 76(4), 503–507. https://doi.org/10.1902/jop.2005.76.4.503

Gupta, A., Kumar, S., Singh, S. K., Kumar, A., Gupta, A., & Mehta, P. (2021). Assessment of Anterior Loop of Inferior Alveolar Nerve and Its Anatomic Variations with Age, Gender, and Dentition Status in Indian Population: A CBCT Study. *International Journal of Dentistry*, 2021, 1–6. https://doi.org/10.1155/2021/1813603

Hm, A., M, S., Ma, A., M, S., & Ma, A. (2012, September 1). *Applications of CBCT in Dental Practice: A Review of the Literature*. General Dentistry. https://pubmed.ncbi.nlm.nih.gov/23032226/

Ibrahim, D., Broilo, T. L., Heitz, C., de Oliveira, M. G., de Oliveira, H. W., Nobre, S. M. W., dos Santos Filho, J. H. G., & Silva, D. N. (2009). Dimensional error of selective laser sintering, three-dimensional printing and PolyJetTM models in the reproduction of mandibular anatomy. *Journal of Cranio-Maxillofacial Surgery*, 37(3), 167–173. https://doi.org/10.1016/j.jcms.2008.10.008

ijsr, K. S. L., Snehal V. Kharwade, Jaykumar R. Gade, International Journal of Science and Research (IJSR). (n.d.). Rapid Prototyping: A Modernistic Era in Prosthodontics, IJSR, Call for Papers, Online Journal. *International Journal of Science and Research* (IJSR). Retrieved December 20, 2023, from https://www.ijsr.net/getabstract.php?paperid=SR20831195638

Jandyal, A., Chaturvedi, I., Wazir, I., Raina, A., & Ul Haq, M. I. (2022). 3D printing – A review of processes, materials and applications in industry 4.0. *Sustainable Operations and Computers*, 3, 33–42. https://doi.org/10.1016/j.susoc.2021.09.004

Kragskov, J., Sindet-Pedersen, S., Gyldensted, C., & Jensen, K. L. (1996). A comparison of three-dimensional computed tomography scans and stereolithographic models for evaluation of craniofacial anomalies. *Journal of Oral and Maxillofacial Surgery: Official Journal of the American Association of Oral and Maxillofacial Surgeons*, *54*(4), 402–411; discussion 411-412. https://doi.org/10.1016/s0278-2391(96)90109-3

Kumar, S. R., Patil, P. G., Choy, C. S., & Veerakumarasivam, A. (2020). The location of the inferior alveolar nerve in the malaysian population: Implications for dental implant planning. *Indian Journal of Dental Research: Official Publication of Indian Society for Dental Research*, 31(2), 197–202. https://doi.org/10.4103/ijdr.IJDR_553_17

Murugesan, K., Anandapandian, P. A., Sharma, S. K., & Vasantha Kumar, M. (2011). Comparative Evaluation of Dimension and Surface Detail Accuracy of Models Produced by Three Different Rapid Prototype Techniques. The Journal of Indian Prosthodontic Society, 12(1), 16–20. https://doi.org/10.1007/s13191-011-0103-8

Safira, L. C., Bastos, L. C., Oliveira, T. B. de, Beal, V. E., Azevedo, R. A. de, & Sarmento, V. A. (2011). Avaliação da fidelidade de biomodelos de prototipagem rápida: estudo experimental in vivo. *ImplantNews*, 161–166. https://search.bvsalud.org/gim/resource/es/lil-599194

Santana, R. R., Lozada, J., Kleinman, A., Al-Ardah, A., Herford, A., & Chen, J.-W. (2012). Accuracy of Cone Beam Computerized Tomography and a Three-Dimensional Stereolithographic Model in Identifying the Anterior Loop of the Mental Nerve: A Study on Cadavers. *Journal of Oral Implantology*, 38(6), 668–676. https://doi.org/10.1563/aaid-joi-d-11-00130

Shahbazian, M., Jacobs, R., Wyatt, J., Willems, G., Pattijn, V., Dhoore, E., Van Lierde, C., & Vinckier, F. (2010). Accuracy and surgical feasibility of a CBCT-based stereolithographic surgical guide aiding autotransplantation of teeth: in vitro validation. *Journal of Oral Rehabilitation,* 37(11), 854–859. https://doi.org/10.1111/j.1365-2842.2010.02107.x

Silva, D. N., Gerhardt de Oliveira, M., Meurer, E., Meurer, M. I., Lopes da Silva, J. V., & Santa-Bárbara, A. (2008). Dimensional error in selective laser sintering and 3D-printing of models for craniomaxillary anatomy reconstruction. *Journal of Cranio-Maxillofacial Surgery*, *36*(8), 443–449. https://doi.org/10.1016/j.jcms.2008.04.003

Singare, S., Lian, Q., Ping Wang, W., Wang, J., Liu, Y., Li, D., & Lu, B. (2009). Rapid prototyping assisted surgery planning and custom implant design. Rapid Prototyping Journal, 15(1), 19–23. https://doi.org/10.1108/13552540910925027

Taft, R. M., Kondor, S., & Grant, G. (2011). *Accuracy of rapid prototype models for head and neck reconstruction*. 106(6), 399–408. https://doi.org/10.1016/s0022-3913(11)60154-6

Viegas, D. M. da C. C. P., Hermínio, J. R. L., Fernandes, J. P., Arrobas, F., Roque, J. C., Mourão, J. T. C. G., & Saavedra, G. de S. F. A. (2021). Trueness and precision of the reproduction of dental casts by the conventional, milling and 3D printing techniques. *Brazilian Dental Science,* 24(4 suppl 1). https://doi.org/10.4322/bds.2021.e2891

Voet, V. S. D., Schnelting, G. H. M., Xu, J., Loos, K., Folkersma, R., & Jager, J. (2018). Stereolithographic 3D Printing with Renewable Acrylates. *Journal of Visualized Experiments*, 139. https://doi.org/10.3791/58177

Volpato N, et al. *Prototipagem Rápida - Tecnologias e Aplicações*. Edgard Blucher, 2007.